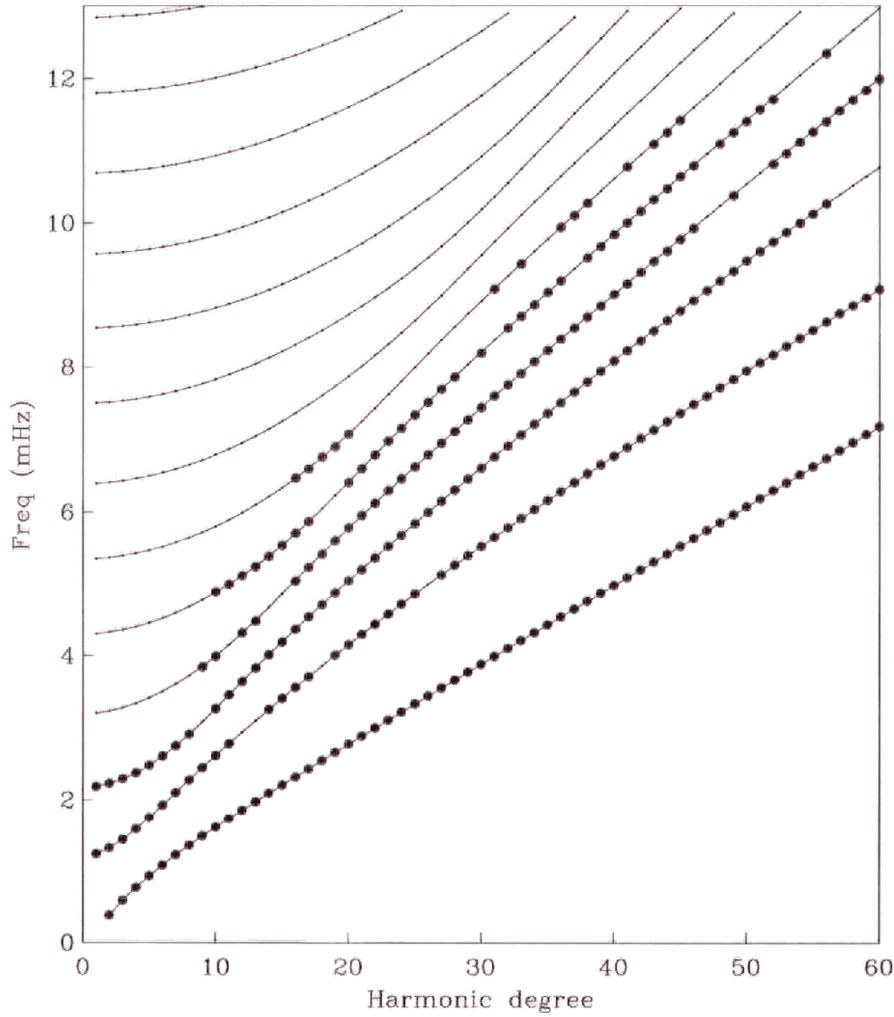


Toroidal \approx JOD observation



Using mode frequencies to make new models - perturbation theory:

$$\frac{\delta \omega_k}{\omega_k} \approx \frac{\delta \sigma_k}{\sigma_k} = \int_0^a \left[K_k(r) \frac{\delta v_p(r)}{v_p} + M_k \frac{\delta v_s(r)}{v_s} + R_k(r) \frac{d\epsilon(r)}{dr} \right] dr$$

+ terms of second order

compute $K_k(r)$, $M_k(r)$ and $R_k(r)$ from eigenfunctions

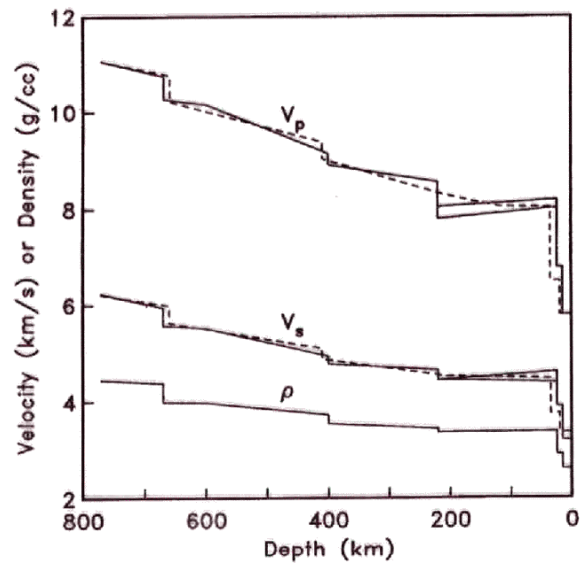
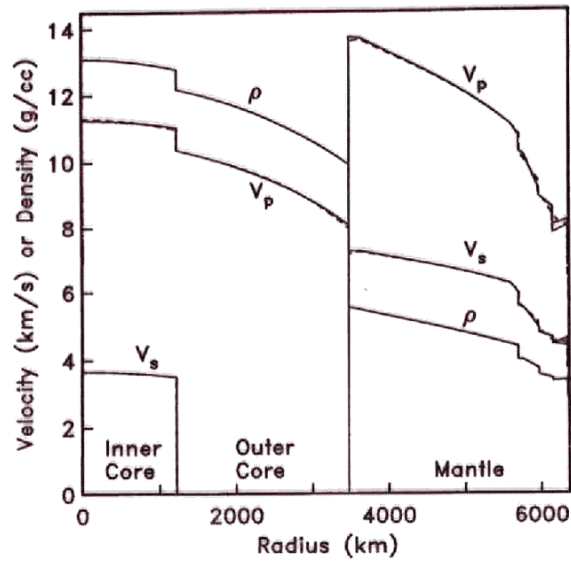


Figure 3.1 Some 1D models of the Earth. The solid lines are (anisotropic) PREM and the dashed line is a variant of IASP91

Resolution ?

$$\delta\omega_k = \int G_k(r) \delta m(r) dr$$

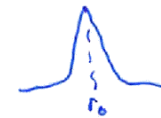
$$\sum a_{ik} \delta\omega_k = \int \sum a_{ik} G_k(r) \delta m(r) dr$$

$\xleftarrow{R(r)}$
 make δ -like

$$\approx \int \delta(r-r_0) \delta m(r) dr = \delta m(r_0)$$

$$= m_E(r_0) - m_0(r_0)$$

In reality, $R(r)$ will be peaked



$$\sum a_{ik} \delta\omega_k = \int \text{peaked } \delta m(r) dr = \overline{\delta m(r_0)}$$

\uparrow local average

has an error since $\delta\omega_k \pm \sigma_k$

Trade off between width of R and error in local average

Linear Resolution Analysis

$$\frac{\delta\omega_k}{\omega_k} \pm \sigma_k = \int_0^a \left[\underbrace{K_k(r)}_{\delta \rho} \frac{\delta V_p}{V_p}(r) + M_k(r) \frac{\delta V_s}{V_s}(r) + R_k(r) \frac{\delta \rho}{\rho}(r) \right] dr + \sum_j A_{jk} \delta h_j$$

> .05%

+ C (unc)

A_j

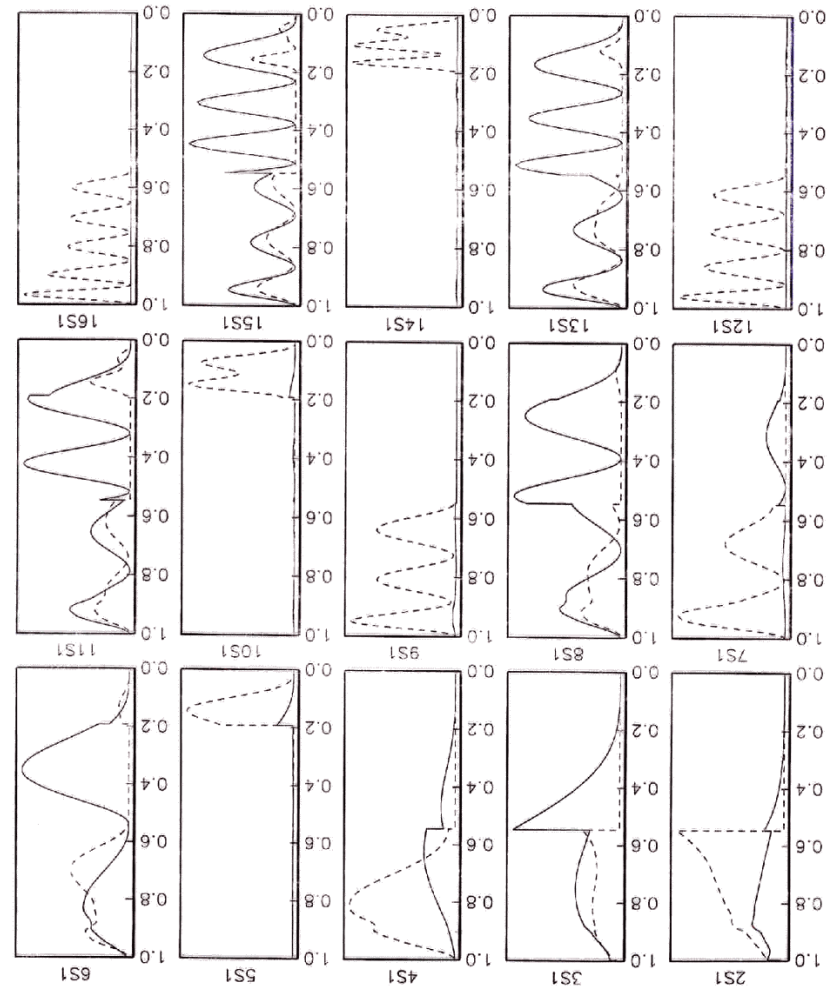
- Take linear combination of data:

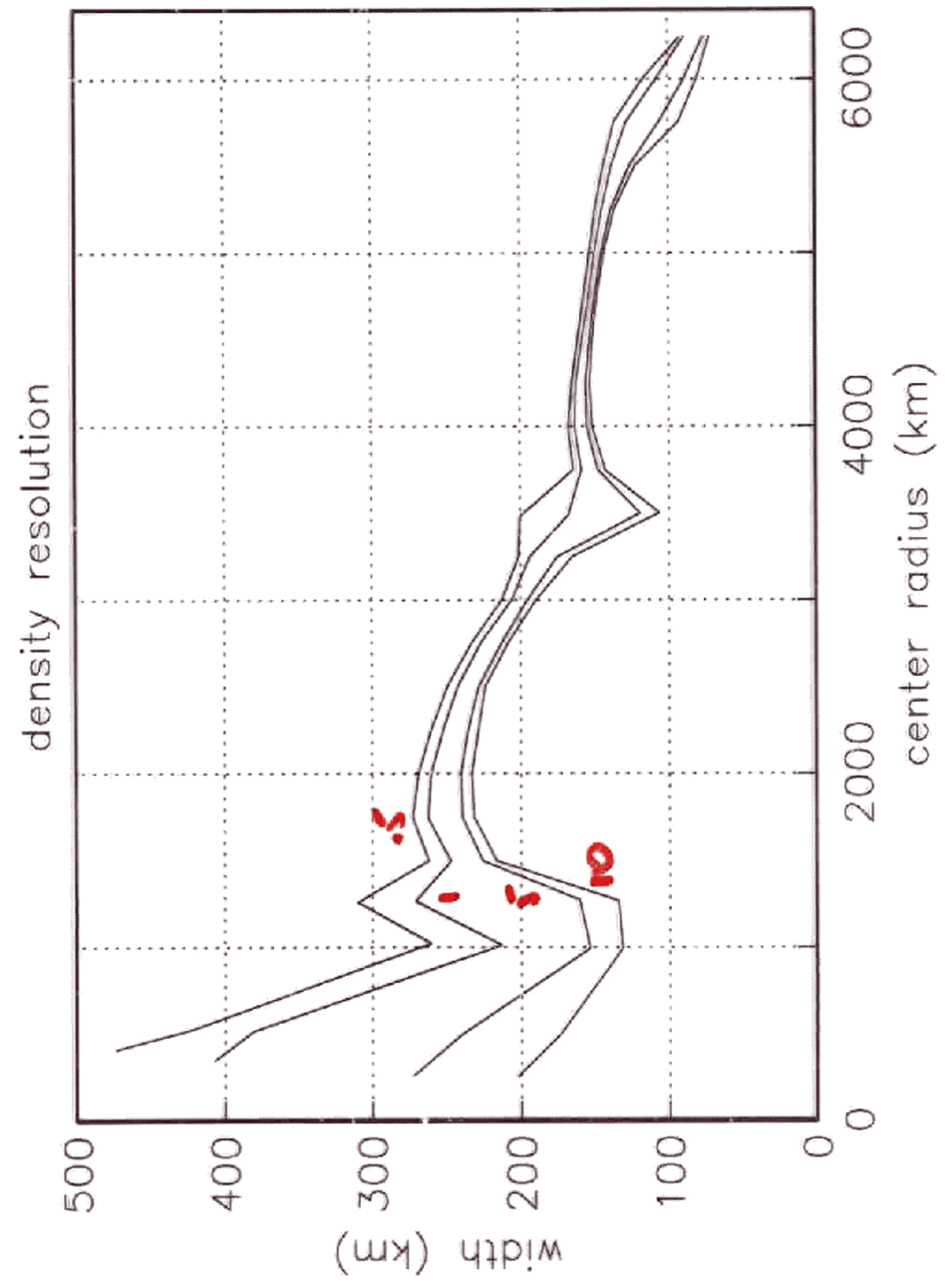
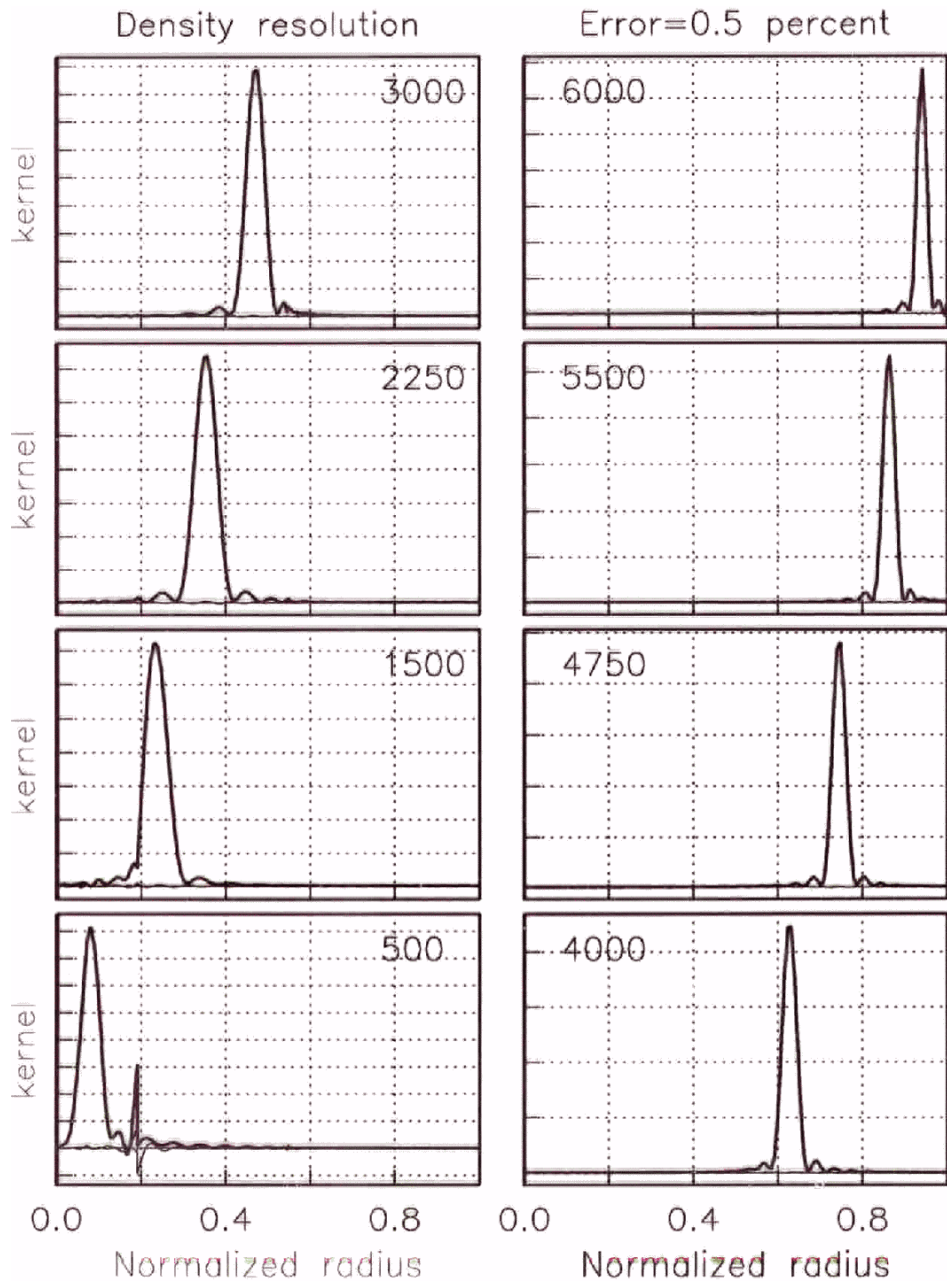
$$\sum_k a_k \frac{\delta\omega_k}{\omega_k} = \int_0^a \left[\mathcal{K}(r) \frac{\delta V_p}{V_p}(r) + \mathcal{M}(r) \frac{\delta V_s}{V_s}(r) + \mathcal{R}(r) \frac{\delta \rho}{\rho}(r) \right] dr + \sum_j A_j \delta h_j$$

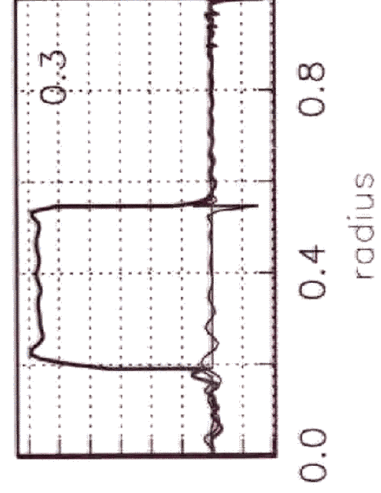
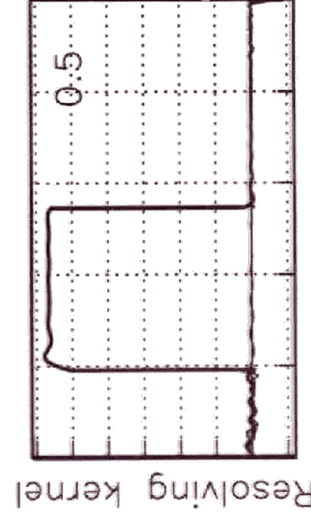
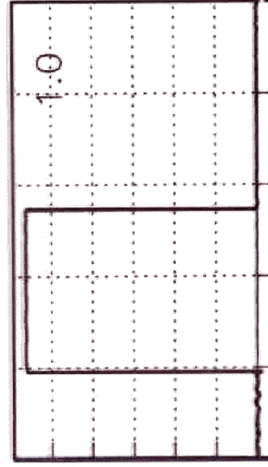
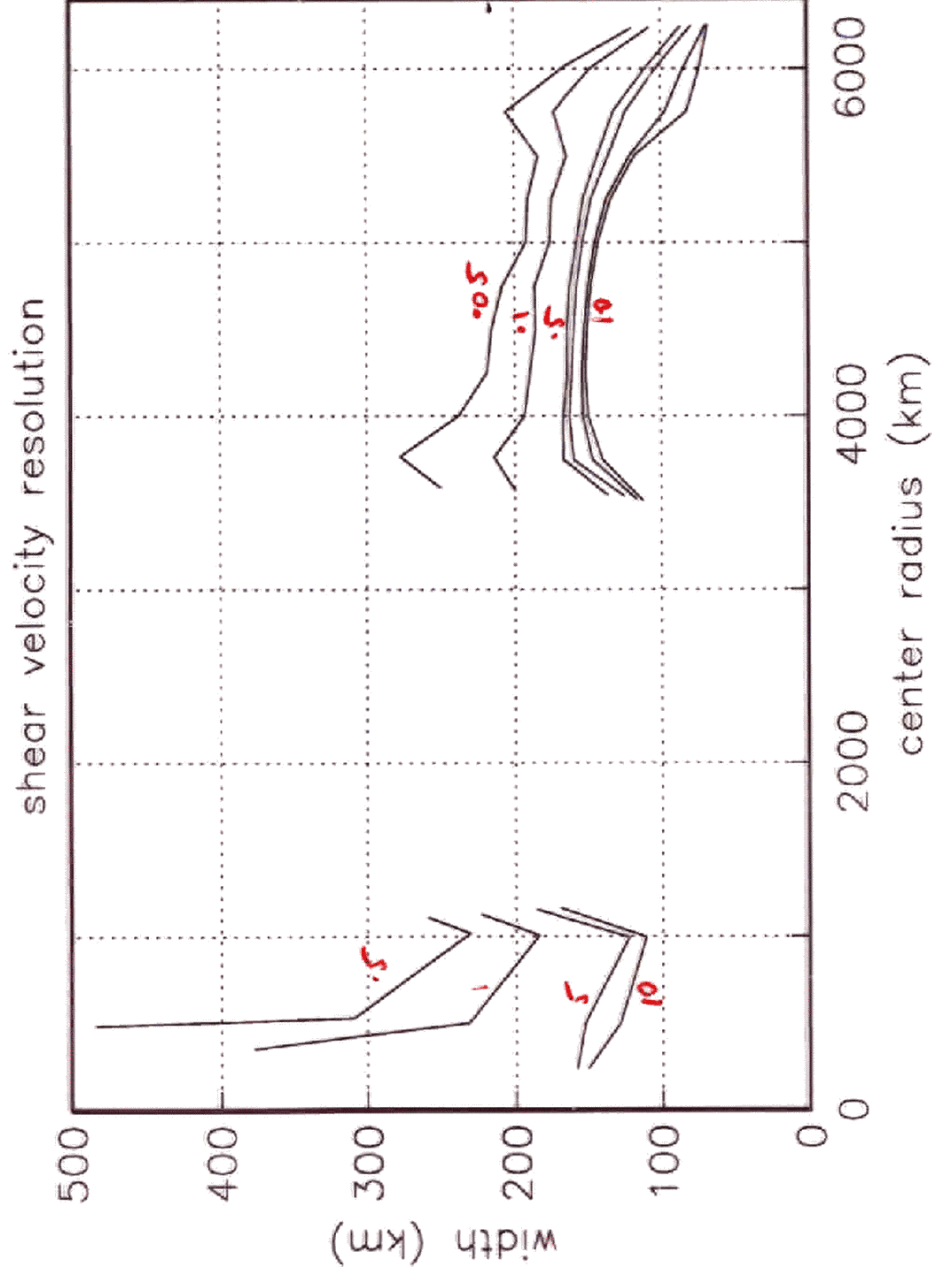
where $\mathcal{K} = \sum_k a_k K_k$, $\mathcal{M} = \sum_k a_k M_k$, $\mathcal{R} = \sum_k a_k R_k$, $A_j = \sum_k a_k A_{jk}$.

- Make \mathcal{R} δ -like and everything else zero.
- Tradeoff with errors

11/15/98 18:39:57







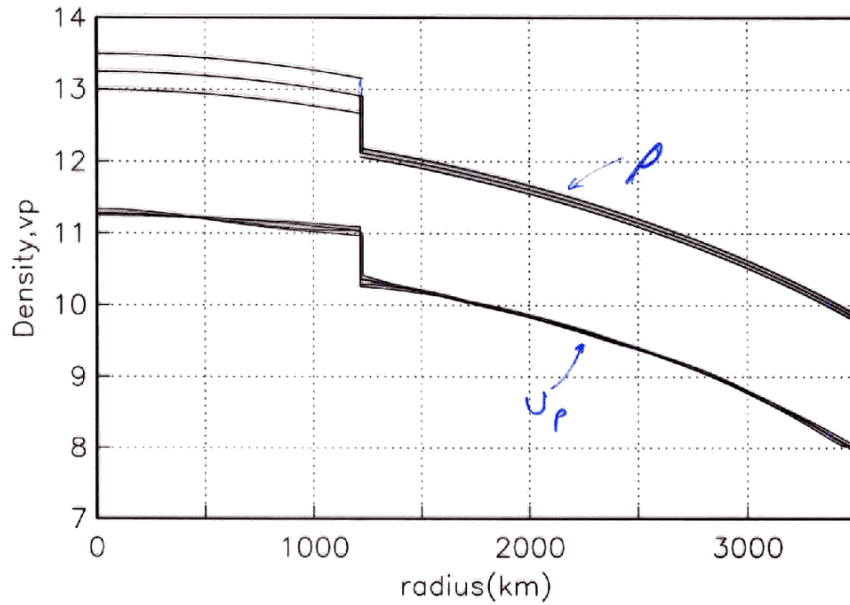
Box car resolution
 kernels for density
 in outer core
 => accurate estimate
 of mass of outer
 core

Adams - Williamson (adiabatic - well mixed)

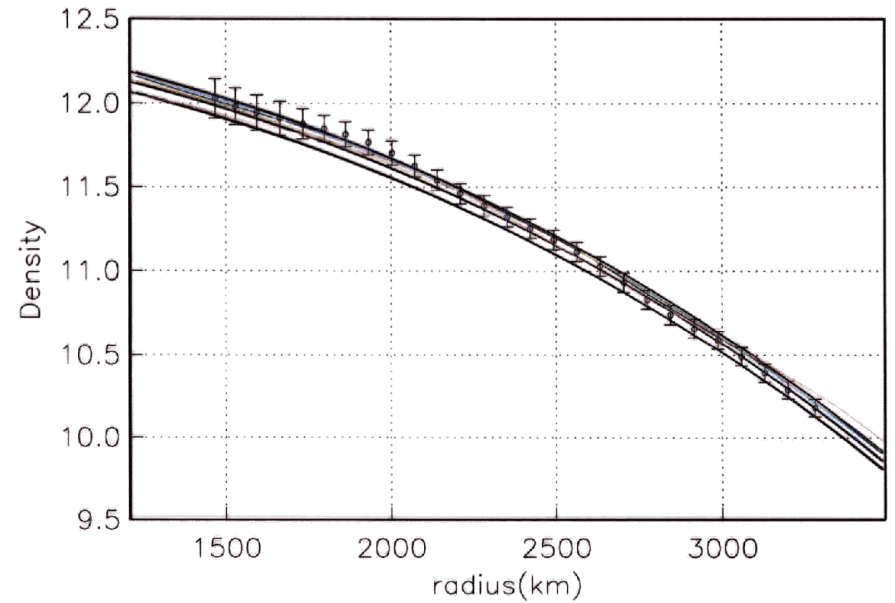
$$\frac{d\rho}{dr} = - \frac{g\rho}{\phi}$$

$$\phi = V_p^2 - \frac{4}{3} V_s^2$$

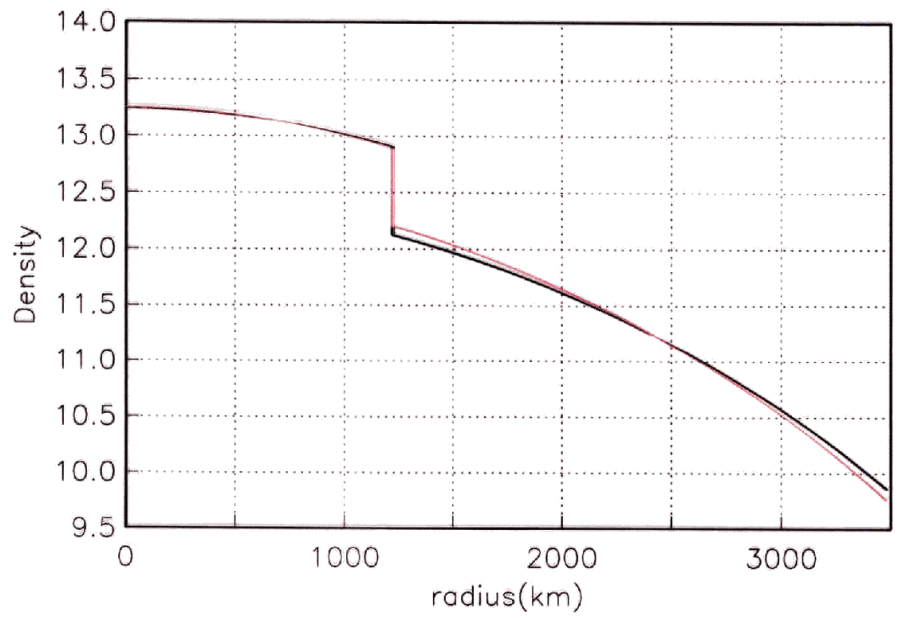
⇒ Can get ρ if know ϕ , mass of core and mass of outer core



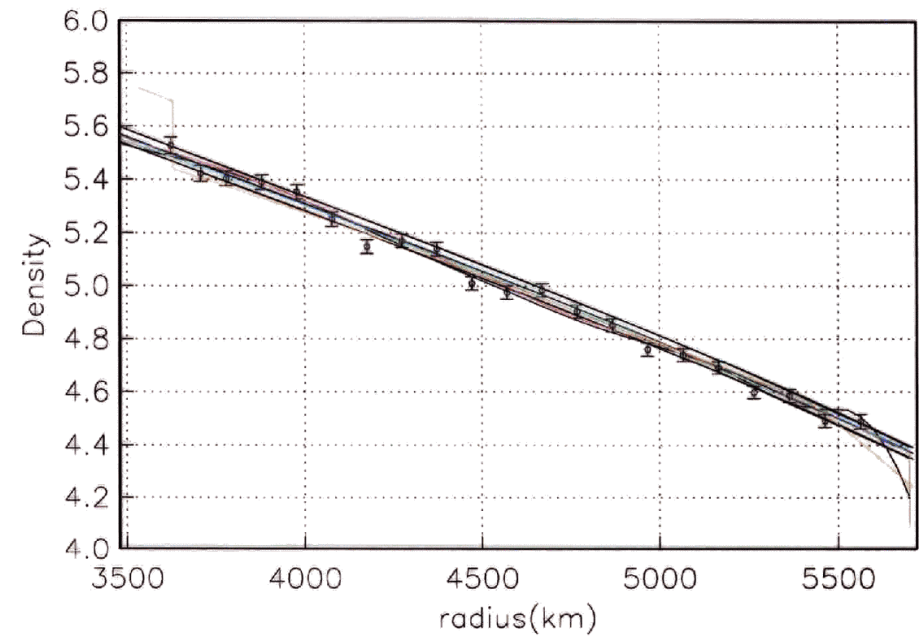
Local averages of density compared with A-W condition.



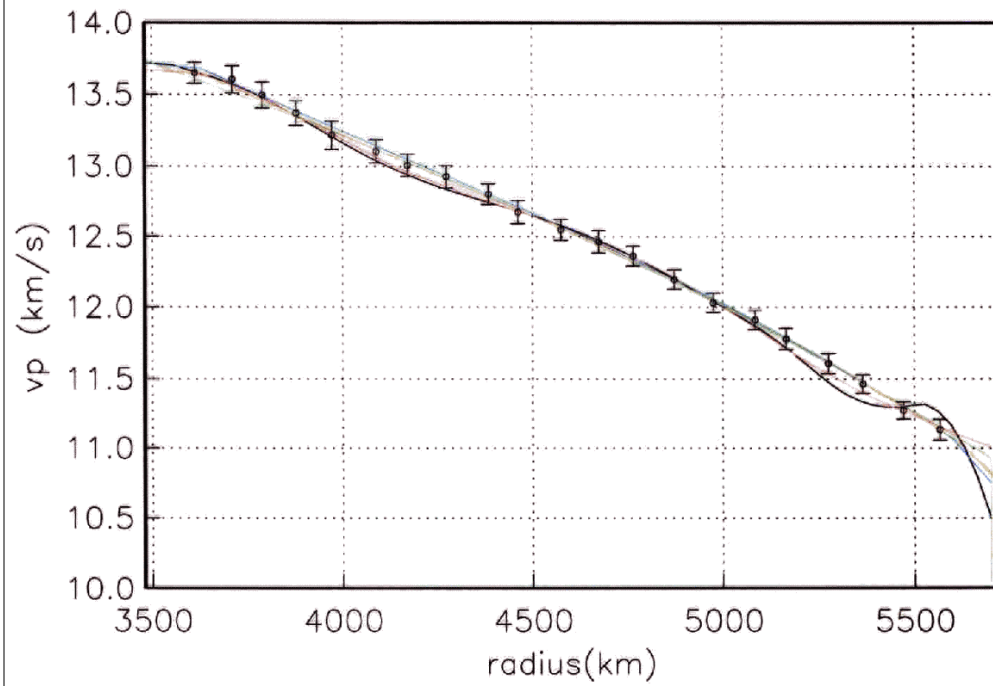
Red line \Rightarrow isothermal outer core



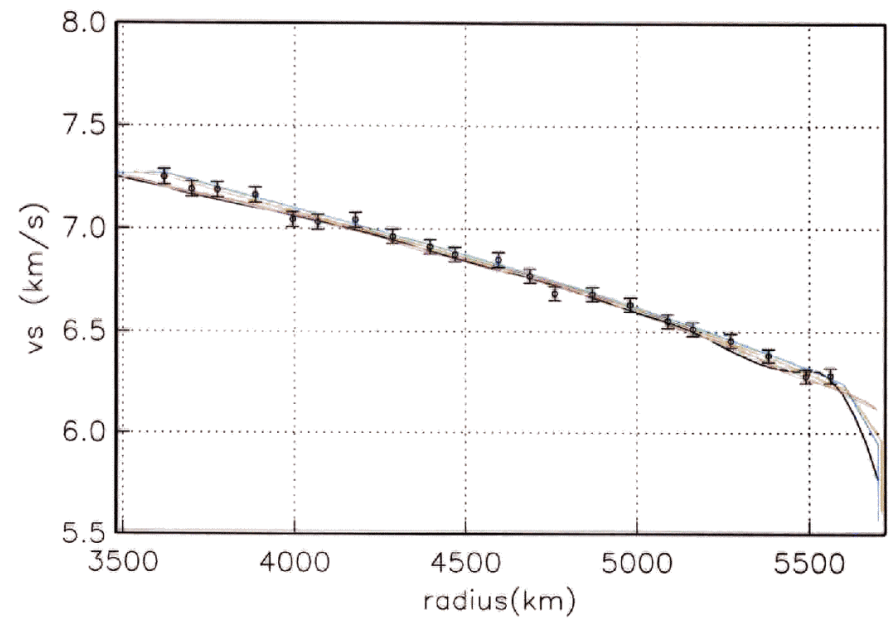
ρ in Lower mantle



v_p in lower mantle



v_s in lower mantle



Resolution results: lowermost mantle

- Mean density of bottom 500km of mantle is $5.465 \pm 0.027 \text{ Mg m}^{-3}$. Mean density of "standard" models is 5.447 Mg m^{-3} . Maybe 0.4% denser though increase is within the observational errors.
- Kellogg et al, 1999 found that a 1% density difference gave a long-lived "hot abyssal layer" with variable upper topography. Our results indicate that this density increase is probably a factor of two too big.
- Would a density excess of 0.4% be enough to give a stable layer?
- Could the layer be much narrower and so not resolvable by the modes?

Resolution results: inner core

- 500km region centered 250km below ICB. With 1% error, density is 12.95 Mg m^{-3} (this is denser than the models which typically have a density of 12.83 Mg m^{-3}).
- 500km region centered 250 km above ICB. With 1% error, density is 11.80 Mg m^{-3} (this is less dense than the models which typically have a density of 12.01 Mg m^{-3}).
- The models typically have a density difference between 1000km and 1500km radius of about 0.84 Mg m^{-3} of which 0.57 Mg m^{-3} comes from the density jump and 0.27 Mg m^{-3} comes from compression effects
- Our analysis gives a density difference of 1.09 Mg m^{-3} leading to a density jump of $0.82 \pm 0.18 \text{ Mg m}^{-3}$.

Attenuation in earth

$$Q_k^{-1} = \int K_k(r) Q_k^{-1}(r) + M_k(r) Q_{\mu}^{-1}(r) dr$$

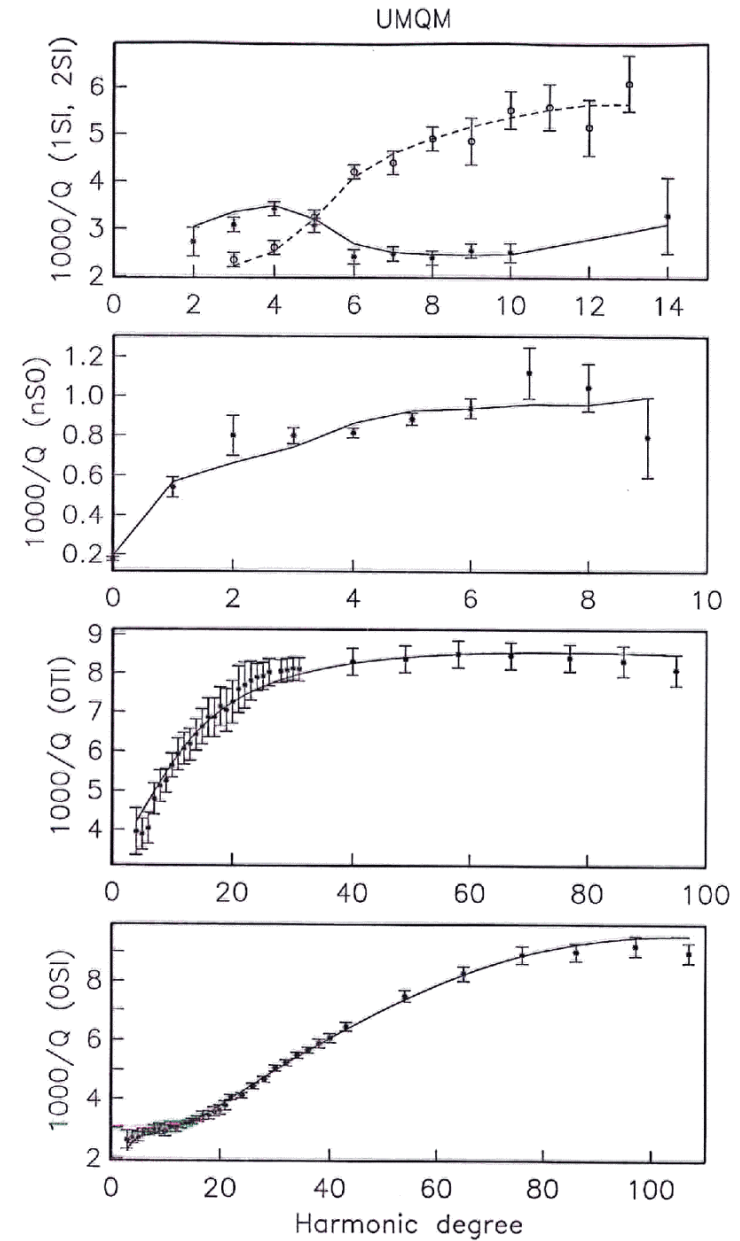
$$\alpha_k = \frac{\omega_k}{2Q_k}$$

$$\omega_k \Rightarrow \omega_k + i\alpha_k$$

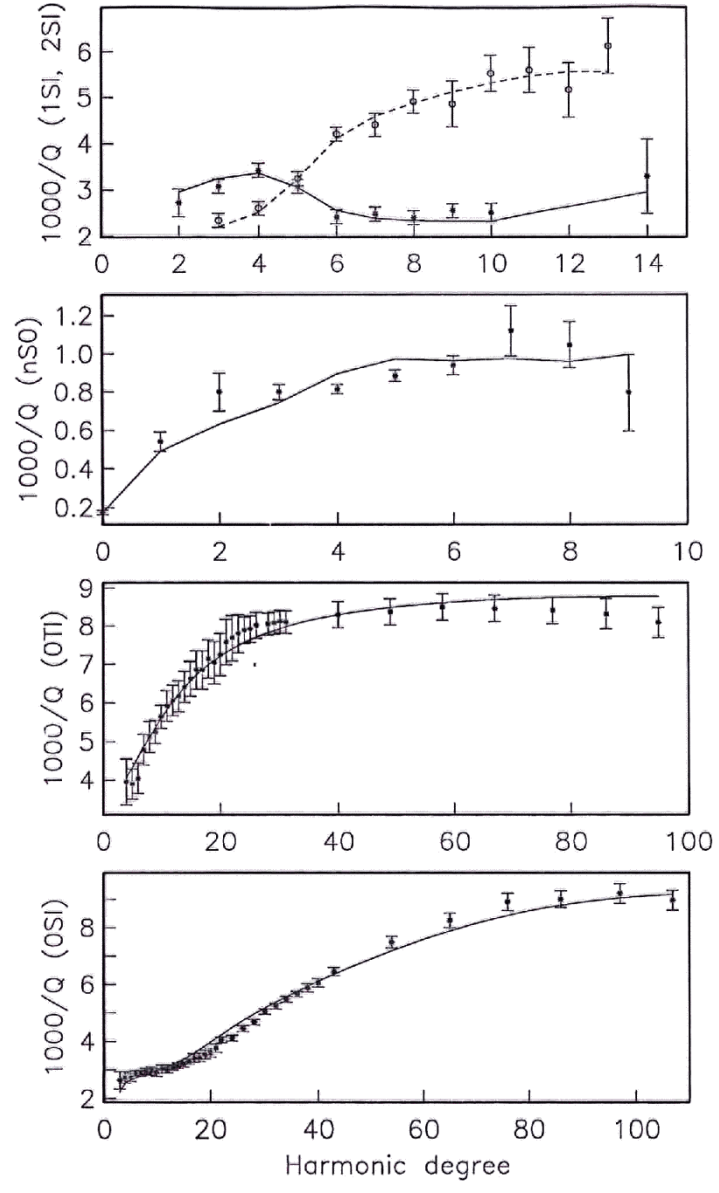
$$K = K_0 \left(1 + \frac{i}{Q_k} \right)$$

$$\mu = \mu_0 \left(1 + \frac{i}{Q_{\mu}} \right)$$

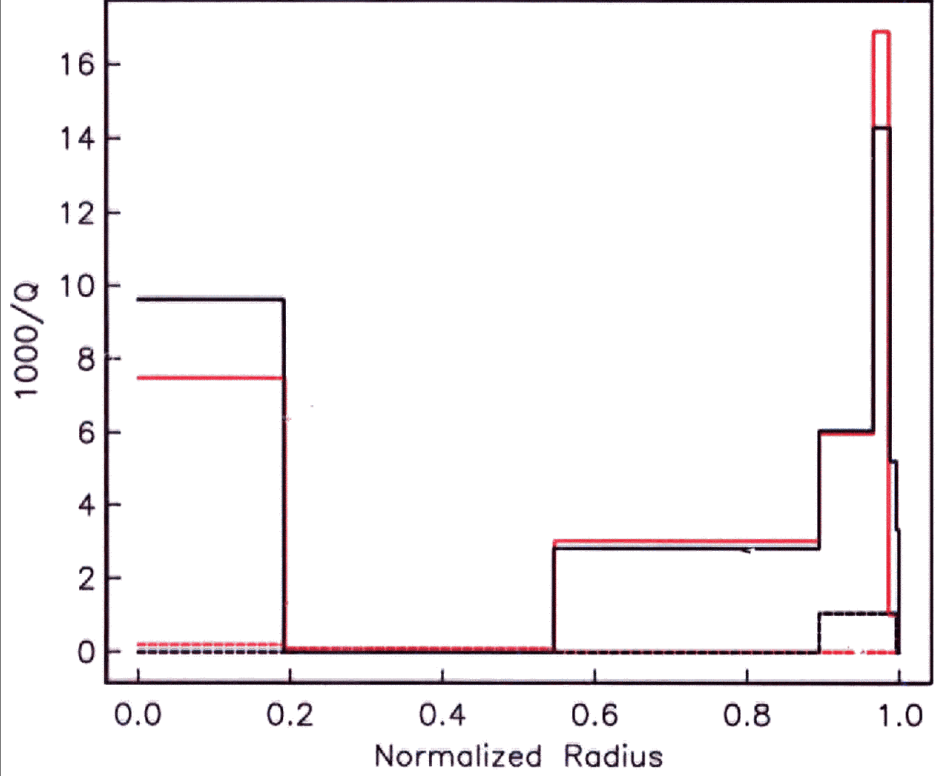
$K_k(r)$ and $M_k(r)$ are compressional and shear energy density (see eqn 11)



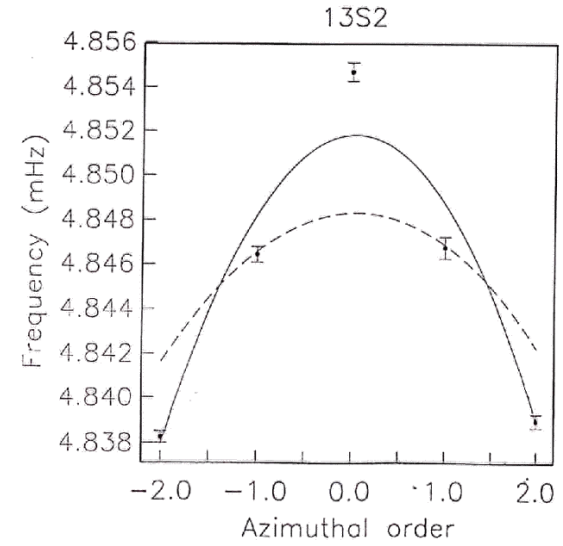
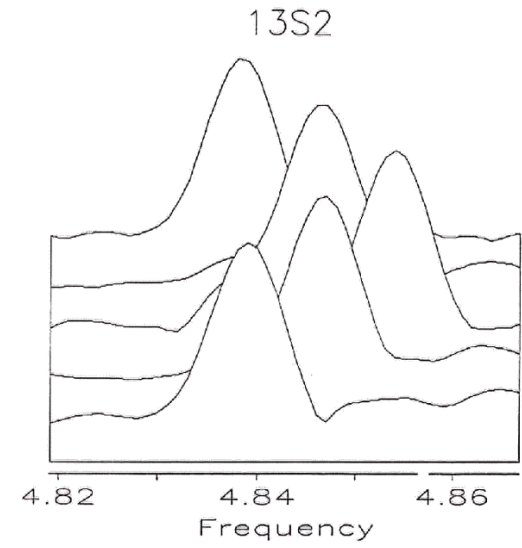
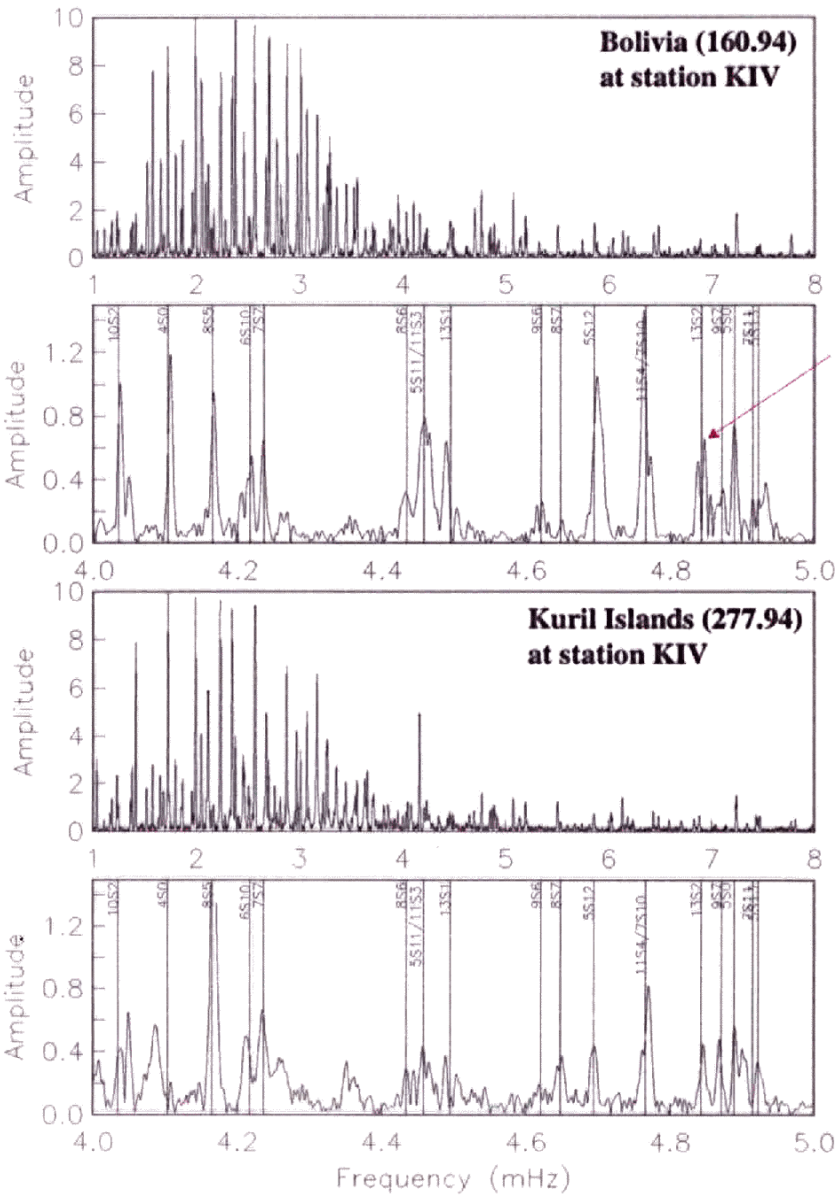
QL6



Q16(black), New(red)



Q_{16} ?
 Q_{21} important in IC and asthenosphere



The splitting matrix

Expand 3D structure in spherical harmonics:

$$\delta \mathbf{m}(r, \theta, \phi) = \sum_{s,t} \delta \mathbf{m}_s^t(r) Y_s^t(\theta, \phi)$$

Let a "structure coefficient" be

$$c_s^t = \int \mathbf{M}_s(r) \cdot \delta \mathbf{m}_s^t(r) r^2 dr$$

where \mathbf{M}_s is a kernel which can be computed for any mode.

- The SPLITTING MATRIX is then given by

$$H_{mm'} = \sum_s \gamma_s^{mm'} c_s^{m-m'}$$

The γ s are geometrical factors related to Wigner 3j symbols and are easily computed.

- The elements \mathbf{H} are linear functionals of 3D structure

Splitting functions used to visualize \mathbf{H}

$$f(\theta, \varphi) = \sum_{s,t} c_s^t Y_s^t(\theta, \varphi)$$

Selection Rule

for the vertical component of an isolated spheroidal mode, i.e.,

$$\mathbf{s}_m = \hat{r} U Y_l^m(\theta, \phi) \quad \text{and} \quad \delta \rho_0 = \sum_{s,t} \delta \rho_s^t(r) Y_s^t(\theta, \phi)$$

Thus

$$\int_V \delta \rho_0 \mathbf{s}_{m'} \cdot \mathbf{s}_m dV = \sum_{s,t} \int_V \delta \rho_s^t(r) U^2(r) r^2 dr \int_{\Omega} Y_l^{m'} Y_l^m Y_s^t d\Omega \quad (5.24)$$

and all three spherical harmonics are functions of θ and ϕ . It is a consequence of the Wigner-Eckart theorem that the splitting matrix $H_{mm'}$ also can be written in the form of 5.24, i.e.,

$$H_{mm'} = \sum_{s,t} \int_V \mathbf{M}_s(r) \cdot \delta \mathbf{m}_s^t(r) r^2 dr \int_{\Omega} Y_l^{m'} Y_l^m Y_s^t d\Omega \quad (5.25)$$

[where \mathbf{M}_s and $\delta \mathbf{m}_s^t$ may be vectors in the sense that they encompass $\delta \rho_0$, $\delta \mu$ and $\delta \kappa$, i.e., $\delta \mathbf{m}_s^t = (\delta \rho_s^t, \delta \mu_s^t, \delta \kappa_s^t)$]. We shall justify the form 5.24 later but, for now, we note that the integral over three spherical harmonics is often zero and we need some special conditions to get a non-zero contribution to a splitting matrix element. These conditions are called *selection rules*.

5.4 Selection rules. Consider the integral

$$\gamma_{sll'}^{mm'} = \int_{\Omega} Y_l^{m'} Y_s^t Y_l^m d\Omega$$

We can separate this into an integral over θ and an integral over ϕ where the integral over ϕ is

$$\int_0^{2\pi} e^{-im\phi} e^{it\phi} e^{im'\phi} d\phi$$

which is zero unless $-m + t + m' = 0$ in which case the integral is 2π . Thus our first selection rule is that $-m + t + m' = 0$ and we note that an axisymmetric structure, $t = 0$, only gives non-zero contributions to the splitting matrix when $m = m'$. The second rule comes from the integral over θ . The product of Y_l^m 's is a polynomial which must not be antisymmetric about the equator otherwise we again have a zero integral. This is achieved if $l + s + l'$ is an even number. In particular, we note that if $l = l'$ (i.e., an isolated multiplet), s must be even. A final rule comes from the fact that modes cannot be sensitive to structure of arbitrarily high harmonic degree. This rule is the "triangle rule" and requires that

$$|l - l'| \leq s \leq l + l' \quad (5.26)$$

For an isolated multiplet ($l = l'$), we thus find that $0 \leq s \leq 2l$. In summary then, we have in addition to 5.26 that

$$l + s + l' = \text{even} \quad (5.27)$$

$$\text{and } t = m - m' \quad (5.28)$$

When $l = l'$ we write

Selection Rules

isolated

l = harmonic degree of mode
 s = " " " structure

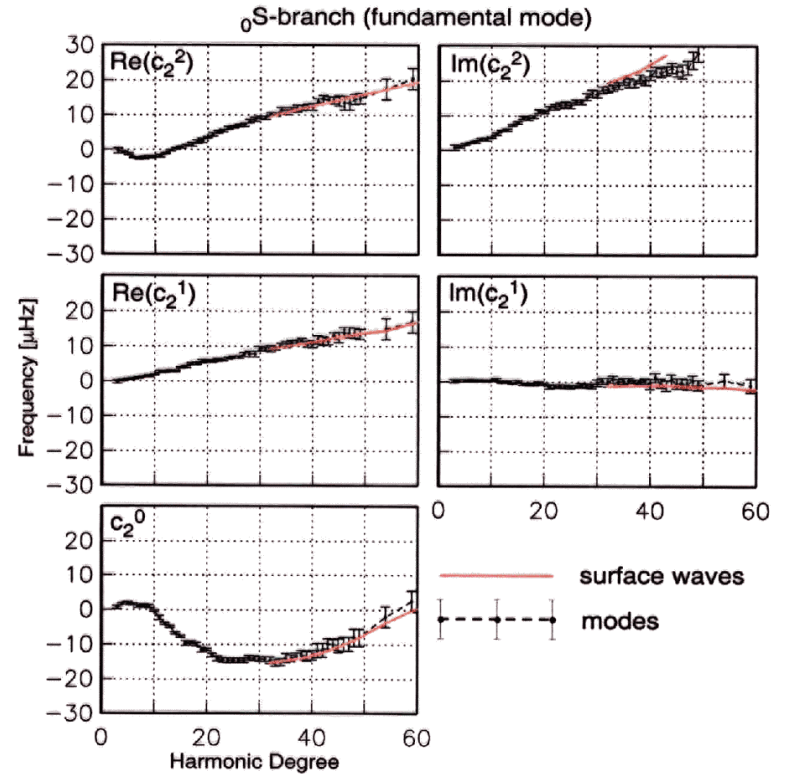
Only sense $0 < s < 2l$

with s even

\therefore $13S_2$ see only $s=2, 4$

* Modes are strong low-pass filters of structure

* Use for looking at long-wavelength structure (and density)



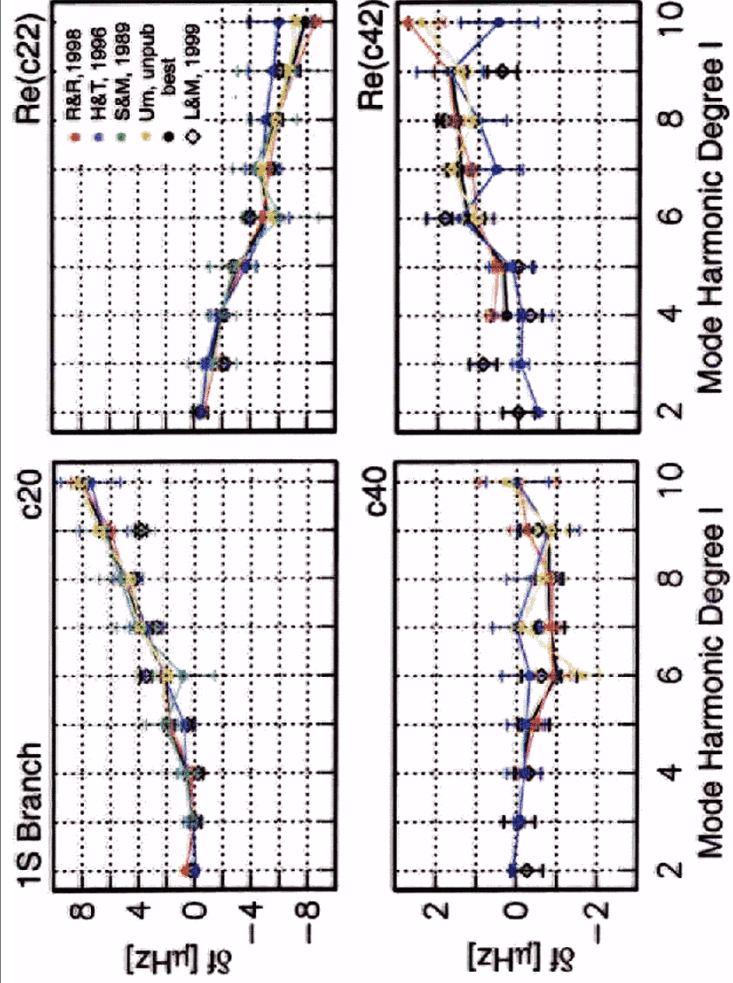
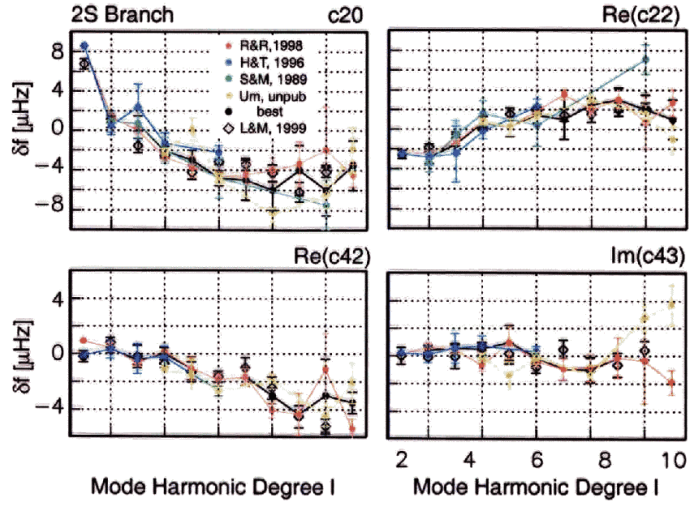
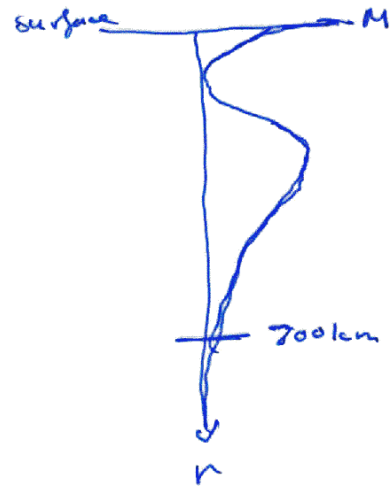
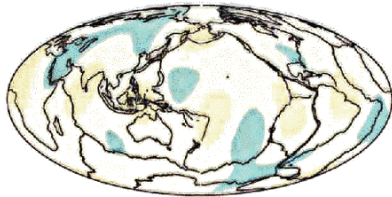


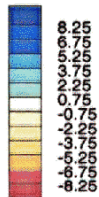
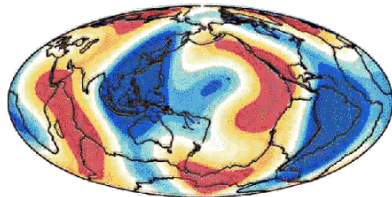
Figure 2. A selection of spheroidal mode structure coefficients for the first overtone branch. Different colors indicate the estimates of Resovsky and Ritzwoller (1998) (red), He and Tromp (1996) (blue), Smith and Masters (1989) (green), unpublished values of Um (yellow) and recent measurements of Laske and Masters (1999) (black diamonds) using the AR method. The black dots denote the "best estimate" which is typically the median of all values. The $s = 2$ coefficients agree well between workers but the $s = 4$ coefficients show considerable scatter.



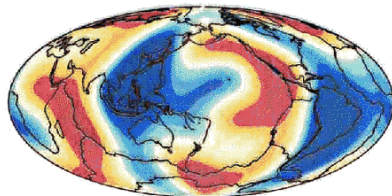
0s20 difference



0s20 synthetic (crust+mantle)



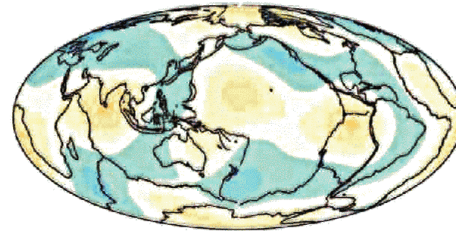
0s20 data



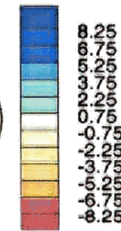
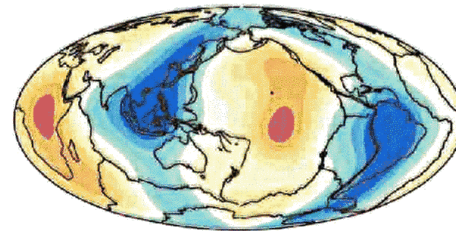
(just 2, 4, 6)

07/29/00 09:54:23

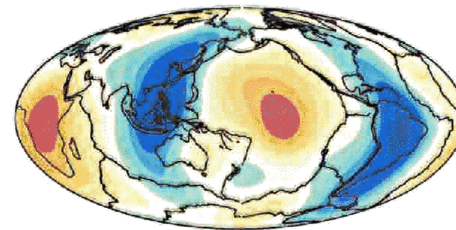
5s8 difference

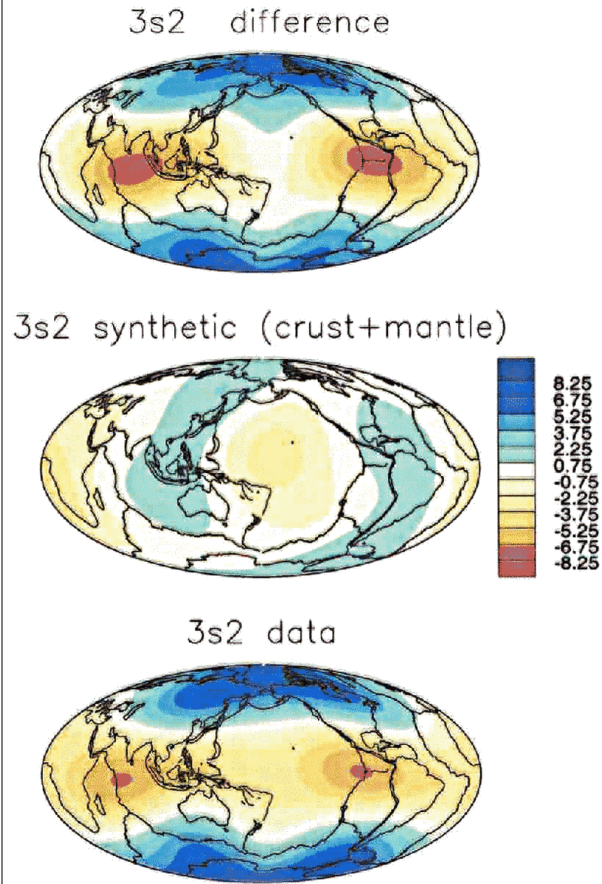


5s8 synthetic (crust+mantle)



5s8 data





07/28/00 17:07:44

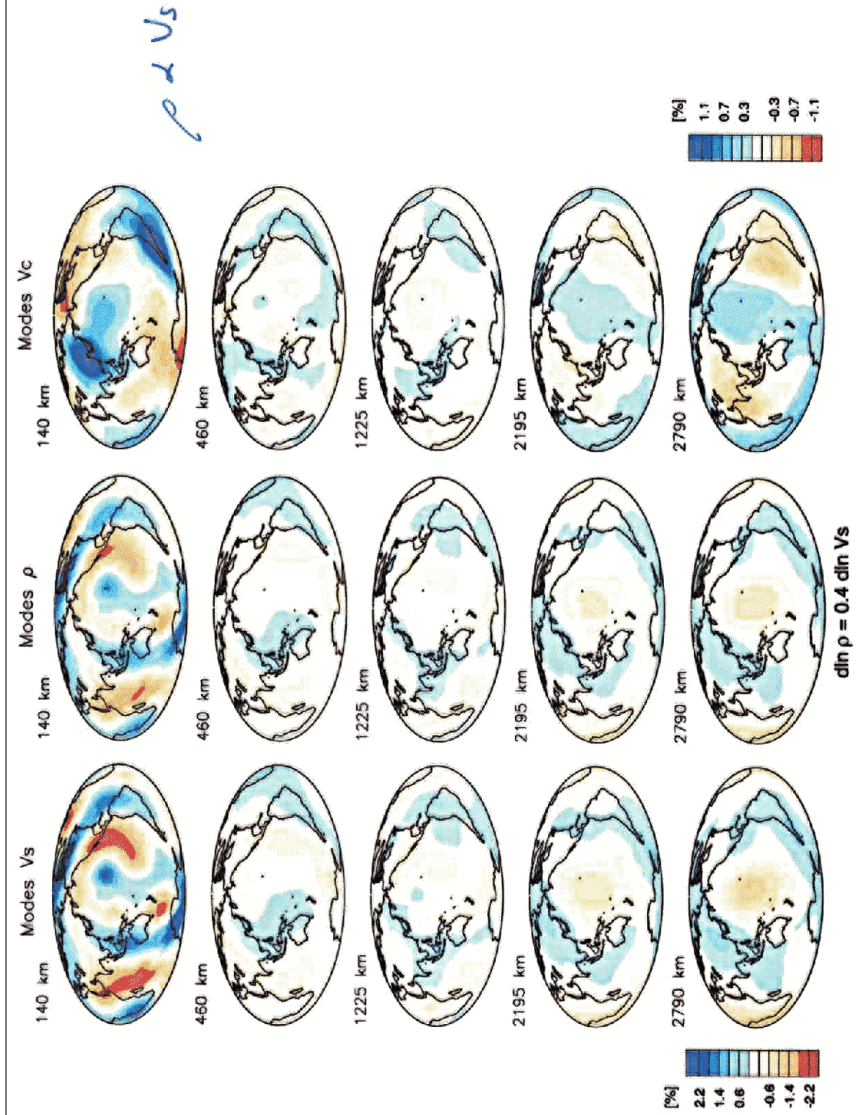


Figure 6. A joint inversion for shear velocity (V_s , left column) and bulk sound speed (V_c , right column) but now with the density being scaled to be proportional to V_s . Note that in both inversions, V_s and V_c are anticorrelated at the base of the mantle. This is a stable feature that is seen in many joint V_c/V_s models (Masters et al., 2000b).

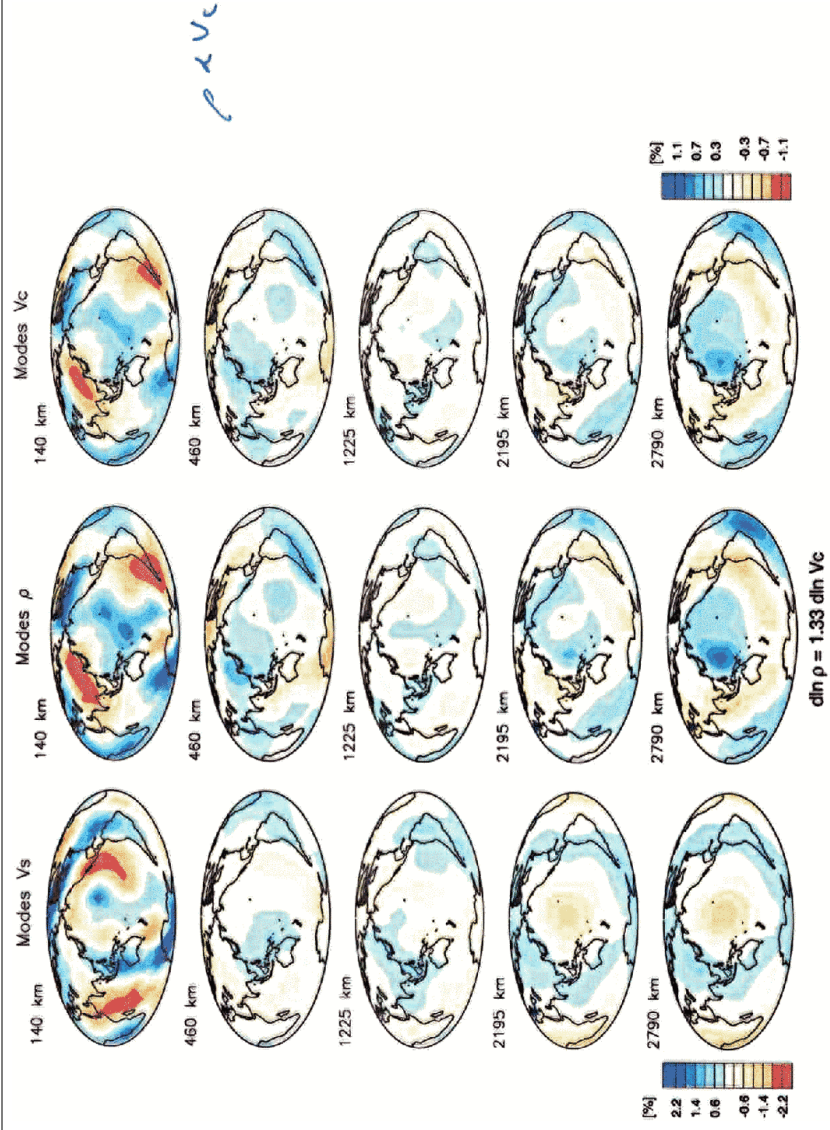


Figure 5. A joint inversion for shear velocity (V_s , left column) and bulk sound speed (V_c , right column) using the “best estimate” structure coefficient data set described in the text and Figures 2 and 3. Each panel shows the relative variation of velocity at a particular depth inside the Earth. Density was scaled to be proportional to V_c and so is negatively correlated to V_s in the lower mantle. The scale of the density variations is the same as that of the variations in V_c , which is half the scale for V_s .

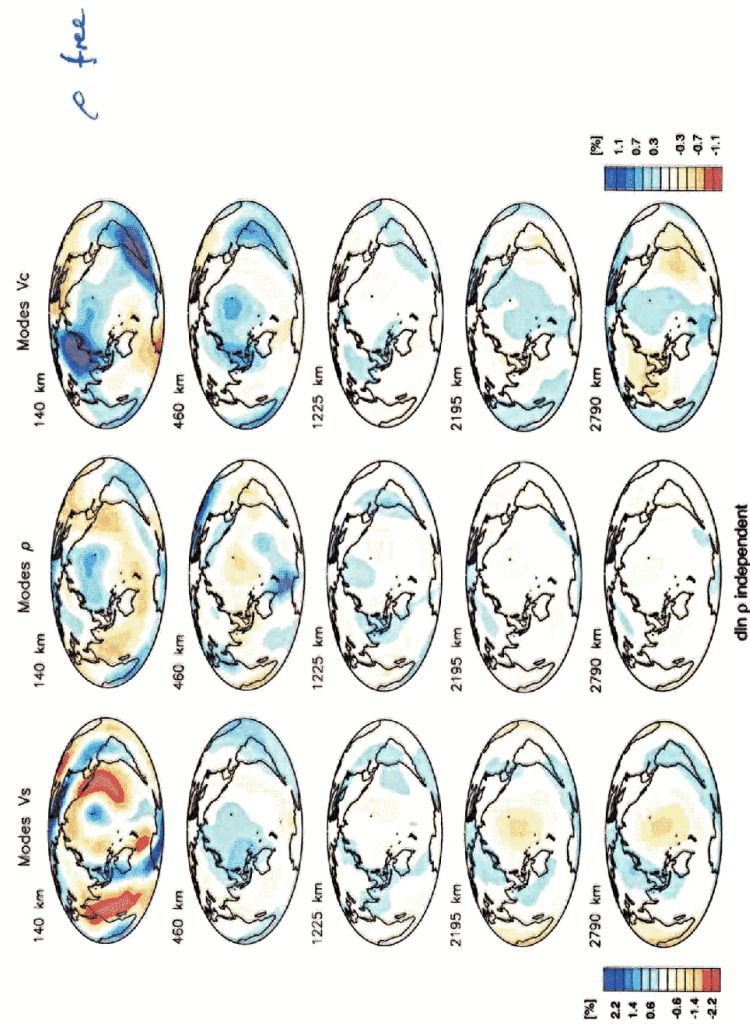
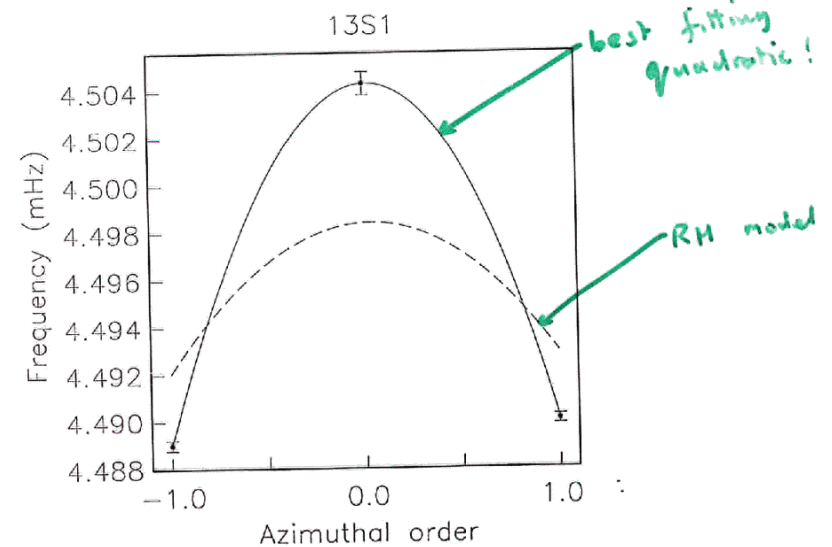
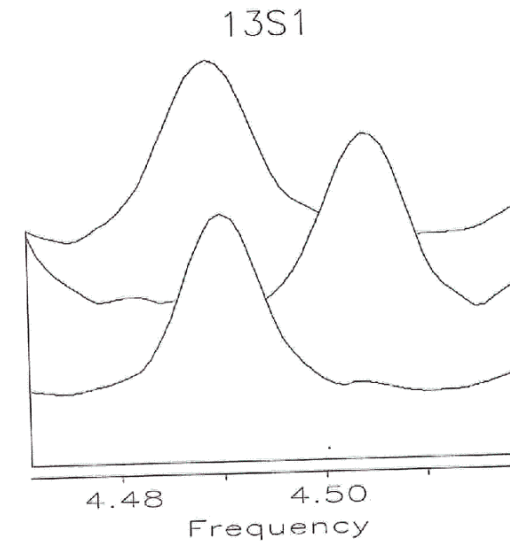
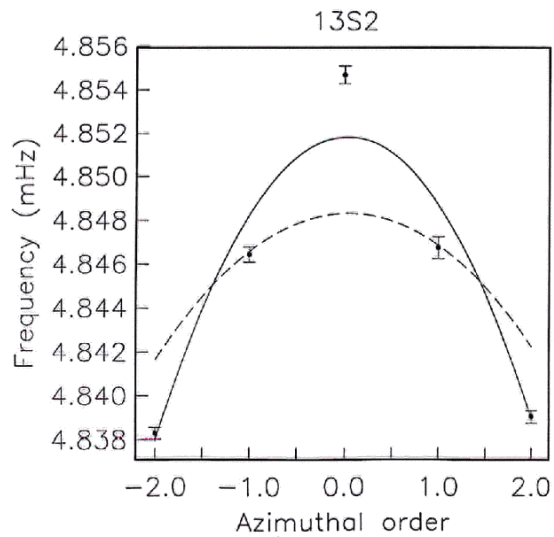
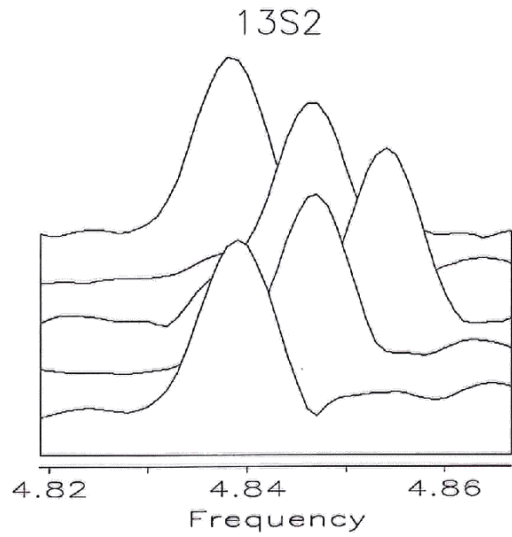


Figure 7. A joint inversion for shear velocity (V_s , left column) and bulk sound speed (V_c , right column) but now the density being solved for independently. In this inversion, as in the two previous ones, V_s and V_c are anticorrelated at the base of the mantle. Also note that density and shear velocity are not anticorrelated at the base of the mantle, which is in contrast to what is found in the recent study of Ishii and Tromp (1999).

Table1 Fit of Density Models to Modes

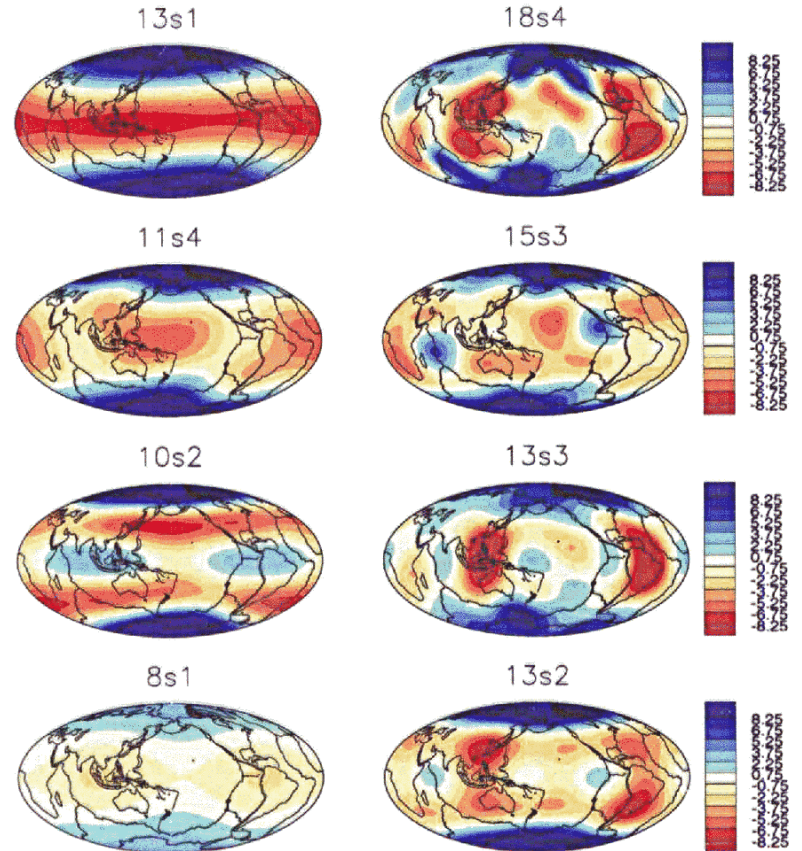
Date set	χ^2/N initial	χ^2/N final	N
Experiment 1: $\delta\rho \sim \delta Vc$			
nS_1 (s=2,4,6)	29.4	0.7	1890
nS_1 (s=2)	93.5	1.4	375
nT_1 (s=2,4,6)	29.1	1.0	810
nT_1 (s=2)	38.5	1.0	215
Experiment 2: $\delta\rho \sim \delta Vs$			
nS_1 (s=2,4,6)	29.4	0.7	1890
nS_1 (s=2)	93.5	1.1	375
nT_1 (s=2,4,6)	29.1	1.0	810
nT_1 (s=2)	38.5	1.0	215
Date set	χ^2/N initial	χ^2/N final	N
Experiment 3: $\delta\rho$ independent			
nS_1 (s=2,4,6)	29.4	0.6	1890
nS_1 (s=2)	93.5	0.9	375
nT_1 (s=2,4,6)	29.1	0.9	810
nT_1 (s=2)	38.5	0.8	215





Corrected for mantle structure

13



14

Energy Densities for the Modes used in this Study

